Available online at www.sciencedirect.com
ScienceDirect
Journal of Molecular Graphics and Modelling 26 (2007) 226–235
Journal of Molecular Graphics and Modelling
www.elsevier.com/locate/JMGM

QSAR study of a large set of 3-pyridyl ethers as ligands of the α4β2 nicotinic acetylcholine receptor

Huabei Zhang [a,*], Hua Li [b], Qinqin Ma [a]

[a] Department of Chemistry, Beijing Normal University, 19# Street Xinjiekou, Beijing 100875, China
[b] Northwest Institute of Nuclear Technology, P.O. Box 69(16), Xi'an, Shannxi 710024, China

Received 12 March 2006; received in revised form 27 November 2006; accepted 28 November 2006
Available online 8 December 2006

Abstract

Extensive 3D-QSAR studies were performed on 158 diverse analogues of 3-pyridyl ethers, which are excellent ligands of α4β2 neuronal nicotinic acetylcholine receptor (NnAChR). Comparative molecular field analysis (CoMFA) and comparative molecular similarity indices analysis (CoMSIA) techniques were used to relate the binding affinities with the ligand structures. Two QSAR models were obtained using CoMFA and CoMSIA techniques. The two QSAR models were proved to be statistically significant and have high predictive power. The best CoMFA model yielded the cross-validated $q^2 = 0.605$ and the non-cross-validated $r^2 = 0.862$. The derived model indicated the importance of steric (85.9%) as well as electrostatic (14.1%) contributions. The CoMFA model demonstrated the steric field as the major descriptor of the ligand binding. The best CoMSIA model gave $q^2 = 0.723$ and $r^2 = 0.685$. This model showed that steric (30.3%) and H-bond interaction (61.8%) properties played major roles in ligand binding process. The squares of correlation coefficient for external test set of 28 molecules were 0.723 and 0.685 for the CoMFA model and the CoMSIA model, respectively. The two models were further graphically interpreted in terms of field contribution maps. SAR studies were also performed on different series of compounds in order to get a more reasonable understanding of the interactions between the ligands and the receptor. With the results, we have also presumed some assistant elements as supplements to the traditional pharmacophoric elements. A crude vision of ligand localization in the ligand-binding pocket of the receptor was also obtained, which would favor for the docking study of this kind of ligands.

Keywords: α4β2; nAChRs; Ligand; Pyridyl ether; 3D-QSAR; CoMFA; CoMSIA

1. Introduction

Nicotinic acetylcholine receptors (nAChRs) represent a family of ligand-gated ion channels distributed throughout the peripheral and central nervous systems (CNS) [1,2]. They include a variety of subtypes, with distinct pharmacological and functional profiles, reflecting the diversity of the genes encoding the five constituent subunits of each receptor. A total of 12 different subunits (2–10 and 2–4) have been identified for neuronal nAChRs (NnAChRs). α4β2 is the most abundant subtype in the mammalian brain and is 95% of the total amount of NnAChRs in the mammalian brain [2,3]. During the past several years, considerable efforts have been directed toward the development of ligands for NnAChRs in the brain. These compounds are of interest because of their potential therapeutic utility in the treatment of central nervous system disorders including Alzheimer's and Parkinson's disease, pain, schizophrenia, anxiety, depression, Tourette's syndrome and smoking cessation [4–8].

Among several classes of α4β2 NnAChR ligands, the most potent ligands are analogues of epibatidine and A-85380 (3-azatidie-methoxyl-pyridine) [8]. However, epibatidine has been limited to be applied in human due to its high toxicity [9]. Compared with epibatidine, A-85380 exhibited a superior selectivity for α4β2 NnAChR and, consequently, an improved in vivo side-effect profile. Currently, the analogues of A-85380 (3-pyridyl ethers analogues) have been becoming the focus in the development of nAChR ligands. A large diversity of 3-pyridyl ether analogues have been synthesized based on bioisosteric substitution in the past decades [10–17]. Some of them evenly obtained an affinity at pM magnitude. In order to search for ligands with higher affinity and specificity, it will be

* Corresponding author. Tel.: +86 10 58802961; fax: +86 10 62200567.
E-mail address: hbzhang@bnu.edu.cn (H. Zhang).

1093-3263/$ – see front matter © 2007 Elsevier Inc. All rights reserved.
doi:10.1016/j.jmgm.2006.11.005

greatly helpful to establish a reasonable pharmacophore model to guide the structural modification in future synthesis of potent ligand.

In the past decades, the QSAR technique has been widely accepted to instruct the synthesis of novel chemicals. QSAR studies have also been investigated on the nAChR [18–24]. However, only a few QSAR studies for 3-pyridyl ethers analogues have been reported. The most comprehensive QSAR study of nAChR ligand performed by Nicolotti et al. [21], 270 various nicotinic agonists, including 62 pyridyl ether analogues, were investigated. By using either a classical Hansch approach or a comparative molecular field analysis (CoMFA), the study revealed detrimental steric effects as the factors mainly modulating the receptor affinity. In 2004, Nicolotti et al. [22] reported another similar QSAR study on 300 nicotinoid agonists by using classical Hansch-type approach, comparative molecular field analysis, and multi-objective genetic QSAR (MoQSAR), a novel evolutionary software that makes use of genetic programming (GP) and multi-objective optimization (MO). In this investigation, additional 58 pyridyl ethers were included, excluding the aforesaid 62 pyridyl ethers. The steric factor was again proved to be the most relevant contributor to the variance of the ligand affinities. We had also carried out a QSAR study on 64 open ring analogues of the pyridyl ethers by using CoMFA, comparative molecular similarity indices analysis (CoMSIA) and molecular hologram QSAR method (HQSAR) [23]. However, the number and classes of 3-pyridyl ethers taken into QSAR investigation in these studies were limited.

A recently stirring achievement in the development of nAChRs ligands is the determination of the three-dimensional molluscan acetylcholine-binding protein (AChBP) at high resolution, which shows significant similarity with the extracelluar parts of the nAChR subunits [25,26]. Based on the protein crystallography, researchers modeled the extracellular domains of α4β2, α3β4 and α7 subtypes and docked a few nicotinic agonists [28–35]. However, few docking researches on pyridyl ether analogues were carried out. QSAR study of diverse pyridyl ether analogues will not only assist in exploring the structural requirements for specific drug design detailedly, but also serve for the docking study of this kind of ligands.

In present study, we performed comprehensive 3D-QSAR analyses using CoMFA technique [36] and CoMSIA technique [37], aiming to deduce some rational guidelines for the structural modification of novel potent ligand with an improved binding affinity to the lead compounds of α4β2 NnAChR. One hundred and fifty-eight diverse compounds of pyridyl ethers were carefully selected to ensure the biological data targeted to the same receptor.

2. Material and methods

2.1. Data set

One hundred and fifty-eight diverse pyridyl ether analogues were taken from several published works [10–13,38–44]. Our study was based on two fundamental

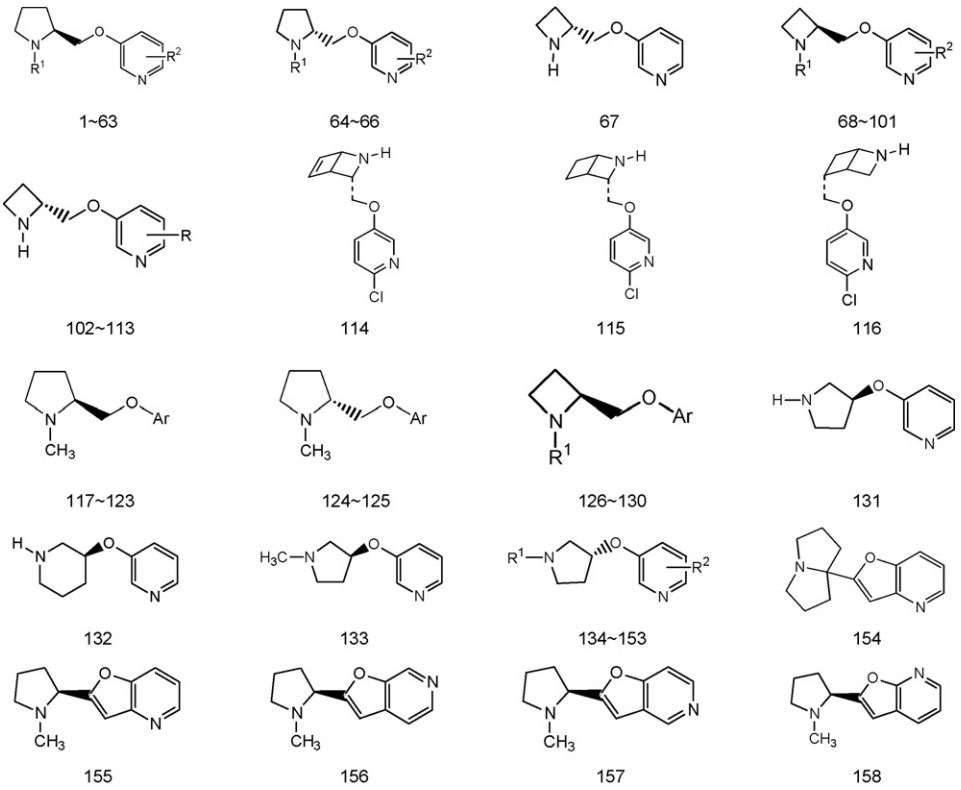

Fig. 1. Structure of ligands in molecular database. R^1 = H or CH_3; r^2 = 2- and/or 4- and/or 5- and/or 6-substitutes. Detailed information about the substitutes is available in supplementary data.

assumptions: (i) all the ligands bind in the same fashion with the receptor and (ii) the affinity data refer to the same receptor subtype, which is α4β2 subtype. Accordingly, the selection criteria of ligands were as following: (i) the structures of all the ligands contained a pyridine ring, a nitric heterocycle and an ether link between them; (ii) the binding affinity data for α4β2 nAChRs (expressed as K_i and IC_{50}) were measured using the same experimental protocol by [^{3}H]-cytisine replacement; (iii) the compounds were pure enantiomers. The affinity values of these compounds were normalized with respected to the K_i value of 0.052 nM for A-85380 [10]. For ligands 131–153, the binding data (IC_{50}) were transformed into K_i values corresponding to IC_{50} values of 1.5 nM obtained for A-85380 [45] using Eq. (1) [19]. The structures and binding data of these ligands were given in Fig. 1 and Table 1 (data of liangds in training set are available in supplementary data). The binding affinity K_i values were converted into pK_i ($-\log K_i$) and used as dependent variables in the CoMFA, CoMSIA analyses. In order to get reliable results, the total molecular database was further divided into training set-130 compounds and test set-28 compounds. The biological data of training set had an even distribution, and spread over a range of seven logarithmic units. The test set was selected to be similar in chemical classes and a range of pK_i values to that of the training set.

Table 1
Experimental values and predicted residues of binding affinity of test set (residues = experimental − predicted)

No.	$K_i \pm$ S.E.M.	Actual pK_i	CoM FA	CoM SIA	Ref.
2	22.9 ± 3.4	7.64	0.61	−0.85	[11]
6	606 ± 21	6.22	0.67	−0.68	[11]
14	0.32 ± 0.06	9.49	0.43	0.18	[11]
21	4.65 ± 0.46	8.33	−0.54	−0.05	[11]
27	2.56 ± 0.42	8.59	−0.47	−0.19	[11]
33	1.1 ± 0.1	8.96	−0.41	−0.42	[13]
34	0.56 ± 0.13	9.25	0.98	1.23	[13]
41	0.082 ± 0.022	10.09	0.45	0.62	[13]
45	4.2 ± 1.9	8.38	−0.98	−0.98	[13]
55	0.24 ± 0.06	9.62	−0.31	−0.22	[13]
65	0.14	9.85	0.77	0.45	[10]
77	2.3 ± 0.3	8.64	0.04	−0.81	[36]
80	0.18 ± 0.06	9.74	−0.48	−0.35	[36]
84	0.047 ± 0.002	10.33	0.11	0.18	[36]
95	1.36 ± 0.06	8.87	0.76	−0.65	[36]
98	0.022 ± 0.005	10.66	0.39	0.58	[36]
100	1.6 ± 0.2	8.8	−0.31	−0.97	[35]
101	0.45 ± 0.02	9.35	0.32	−0.48	[36]
105	0.053 ± 0.009	10.28	0.57	0.22	[36]
112	0.4 ± 0.007	9.4	−1.23	−0.78	[36]
114	14	7.85	−1.56	−1.17	[37]
118	7914 ± 26	5.91	−1.07	−0.12	[12]
123	29 ± 3	7.54	−0.06	0.11	[12]
141	63.09	7.2	−1.64	−1.39	[38]
142	2.6	8.59	0.2	0.76	[38]
146	0.76	9.12	1.08	0.75	[38]
156	207	6.68	−0.35	−1.71	[40]
157	1700	5.77	−1.02	−0.75	[40]
r^2_{pre}			0.723	0.685	

Notation: r^2_{pre}, square of correlated coefficient of predicted value of all molecules in test set. S.E.M., $n \geqslant 3$. Experimental values and predicted residues of binding affinity of training set are available in supplementary data.

$$K_i = \frac{IC_{50}}{1.5} \times 0.052\,\text{nM} \quad (1)$$

2.2. Molecular modeling

All modeling works were performed using Sybyl 6.91 software package [46]. As currently accepted, the protonated nitrogen as an important pharmacophoric element of NnAChRs ligands [18], the protonated forms of ligands were used in this QSAR study. Consulting the orientation of the proton in the semirigid ligand 154, the protons were added proximal to the pyridine rings in all the ligands. The initial geometry of each compound was optimized using standard Tripos Force Field loaded gasteiger-huckel charge using conjugated gradient method with an energy convergence criterion of 0.001 kcal/(mol Å^2). Then a systematic conformation search was performed on the preliminary optimized structure. For the compounds with flexible bond, the increments of a 10° from 0° to 360° for the selected rotated bond were used in the systematic conformation search. The low-energy conformer with a $\Delta E < 3$ kcal/mol above the global minimum energy conformer of each compound, which gave the best fit to the template molecule, was selected as the possible active conformation. The selected conformation was further optimized using semi-empirical method MOPAC with AM1 Hamiltonian. The final optimized structure with AM1 charges was used for the next alignment.

2.3. Database alignment

The key of alignment is to select a suitable template structure. A ligand structure from crystal ligand–receptor complex or a structure of a rigid ligand with a high affinity was best choice of a template structure. Unfortunately, there had no crystal complex structure for pyridyl ethers. Moreover, several modelling studies of nicotinic ligand have shown that binding modes of diverse series of ligands were different in the ligand binding domain of nAChR [26,27,31,32]. Thus, the rigid cytisine or other classical nAChR ligand was not suitable to use as a template structure for pyridyl ethers. To obtain a reasonable alignment, we finally chose the well-fitted low-energy conformers of semi-rigid compound 154 and high affinity compound 97 as alignment templates.

Pharmacophoric elements alignment was used to investigate additional potent interaction mode between the ligand and the receptor. However, the definitive pharmacophore model is still unclear for pyridyl ethers. Currently accepted pharmacophoric elements of the nicotinic ligand are: the pyridyl nitrogen as H-bond acceptor, the pyridyl centroid as center of hydrophobic interaction and the protonated pyrrolidinyl nitrogen as H-bond donor site or as cation-π interaction site by interacting with a π cloud of aromatic residues on the receptor [21,47]. To obtain a reasonable alignment, we used these pharmacophoric elements as the reference atoms for alignment: (i) the basic nitrogen of the pyridine ring, (ii) the centroid of the pyridine ring, (iii) the

sp^3-hybridized nitrogen atom of the heterocycle and (iv) the proton added to the nitrogen of heterocycle. The molecular alignment used for the study was obtained by means of Fit Atom protocol in Sybyl 6.91 software package. Fig. 2 showed the stereogram of the satisfying alignment of all the molecules (including the test set).

2.4. Calculation of CoMFA and CoMSIA descriptors

In the CoMFA calculation, the aligned molecules were placed in a 3D cubic lattice with default 2 Å spacing. The default sp^3 carbon atom with +1 charge was selected as the probe atom for the calculations of the steric (Lennard–Jones 6–12 potential) and electrostatic fields (Coulombic potential) around the aligned molecules with a distance-dependent dielectric constant at all lattice points. The column filtering was set to 2.0 kcal/mol. Values of steric and electrostatic energies were truncated at 30 kcal/mol. The same grid was also used in the CoMSIA field calculation [36,37]. Five physicochemical properties (steric, electrostatic, hydrophobic, hydrogen bond donor and hydrogen bond acceptor properties) were evaluated using the probe atom. A probe atom sp^3 carbon with charge +1, hydrophobicity +1 and H-bond donor and acceptor property of +1 was placed at every grid point to measure the electrostatic, steric, hydrophobic, H-bond donor and H-bond acceptor field. Different from the CoMFA, a Gaussian type distance dependence of physicochemical properties was used in CoMSIA. The default value of 0.3 was used as the attenuation factor (R).

2.5. A partial least squares (PLS) analyses

CoMFA and CoMSIA models have been derived from a training set of 130 nAChRs ligands. The method of PLS regression was used to correlate variations in the biological activities with variations in the respective descriptors.

Cross validation was undertaken using the Leave One Out (LOO) procedure SAMPLS [48] implemented in Sybyl 6.91 software package. The optimal number of components was determined in such a way that each additional component should increase the q^2 by at least 5% [49]. With the optimized number of components, a non-cross-validation was performed to establish the model for predicting the affinities of compounds in the training set and test set. Progressive scrambling program [49] was performed to test the sensibility of the model to the chance correlation, which gauged by parameter $dq^{2'}/dr^2_{yy'}$—the slope of q^2 (as originally determined using SAMPLS [48]) with respect to the correlation of the original biological activity versus the scrambled biological activity. In a model, if the correlation of activity is not due to chance correlation, the slope will be equal to or less than 1 [49]. Group cross-validation (10 groups) on whole database was also performed to test the robustness of the obtained models.

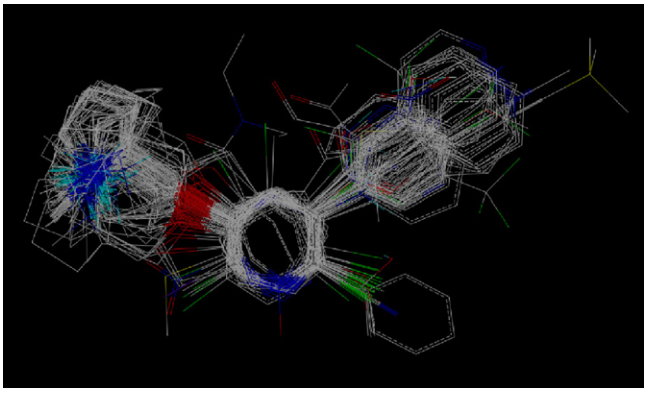

Fig. 2. Stereogram of aligned molecules in the training set and test set.

3. Result and discussion

3.1. CoMFA and CoMSIA models

The models generated by CoMFA and CoMSIA techniques are summarized in Table 2. The best models were selected based on better values of S_{press}, cross-validated q^2, non-crossvalidated r^2 and the standard deviations (S.D.) values.

A CoMFA model contained steric and electrostatic fields was obtained, which provided satisfied values of q^2 (0.605) and r^2 (0.862) with number of optimum component (NOC) = 6. The standard error of prediction was 0.469. The contribution of steric field was predominant and accounted for 85.9% of the reasons of the total affinity changes. This was well agreement with the study of Nicolotti et al. [21,22], whose studies including 256 or 300 various nAChR ligands suggested that the steric effect was the most relevant contributor to rationalize the ligand–receptor interaction.

For CoMSIA analysis, descriptors of five physicochemical field properties were used to correlate with the changes of ligands affinities. To our surprise, the hydrophobic property was found little relate with the changes of the binding affinities, with q^2_{LOO} value about 0.04 and 1 component. The combination of steric and electrostatic properties could not

Table 2
Statistical results of different model derived from training set molecules

	CoMFA	COMSIA		
	S, E	S, E	D, A	S, E, D, A
Statistical result				
q^2	**0.605**	0.467	0.543	**0.603**
S_{press}	**0.793**	0.913	0.845	**0.791**
r^2	**0.862**	0.692	0.744	**0.836**
F	**127.88**	70.192	90.749	**126.623**
S.D.	**0.469**	0.694	0.633	**0.508**
Component	**6**	4	4	**5**
Fraction (%)				
Steric	**0.859**	0.375		**0.117**
Electrostatic	**0.141**	0.625		**0.195**
Donor			0.491	**0.308**
Acceptor			0.509	**0.308**

Notes: S, E: Steric and Electrostatic fields; D, A: Hydrogen donor and Hydrogen acceptor fields; q^2: square of cross-validated correlated coefficient from LOO analysis; r^2: square of non-cross-validated correlated coefficient; S.D.: standard error of prediction; F: value of F-test which denotes ratio of r^2 explained to unexplained $r^2/(1-r^2)$.

Table 3
Group cross-validation results of different models

Model	CoMFA	CoMSIA		
	S, E	S,E	DA	S, E, D, A
Average of q^2	**0.639**	0.481	0.570	**0.640**
Standard deviation of q^2	**0.013**	0.019	0.017	**0.022**

give satisfying models with q^2 values about 0.467, while the cooperation of the H-bond donor and the H-bond acceptor properties gave satisfying statistics with q^2 values of 0.543. When analyzed with combined descriptors of steric, electrostatic and H-bond filed properties, a more significant CoMSIA model was obtained ($q^2 = 0.603$, $r^2 = 0.836$). Moreover, the model comprised of steric, electrostatic and H-bond fields also exhibited the lowest S_{press} and S.D. values in three CoMSIA models. This model (boldfaced in Table 2) was selected as the final CoMSIA model for prediction. The contributions of different field properties to the model were list in Table 2. The H-bond interactions were demonstrated to be the prevalent factors modulating nAChR ligand binding, which explained the 61.8% of the affinity variance. This result was coincident with the popular accepted nicotinic pharmacophore model [21,47], in which a positively charge nitrogen atom and a lone pair of the pyridine nitrogen on the ligand both acted as H-bond site. Thus, the H-bond properties contributed a majority of the stability in the ligand–receptor complex. However, the field contributions of the final CoMSIA model seemed differing from that of the final CoMFA model, where detrimental steric effects acted as the factor mainly modulating the receptor affinity. We assumed that the direction of the H-bond might play a much more important role than the distribution of the electronic density in the CoMSIA analysis. Possibly, CoMFA and CoMSIA models each accounted for a different aspect of the ligand–receptor interactions. The combination of the two models might be the best way to extrapolate the affinity of an external ligand.

To test the stability and reliability of the obtained models, group cross-validation PLS (10 group), as well as progressive scrambling test, were carried out. The group cross-validation was performed on the whole database 20 times (Table 3). The obtained average of q^2_{LNO} was in the similar range as that of the selected models (boldfaced in Table 3), 0.639 for CoMFA and 0.640 for CoMSIA, respectively. The standard deviations in the q^2_{LNO} values from the group cross validation were minimal (0.013 and 0.022 for the final CoMFA and CoMSIA models, respectively), which indicated that stability and robustness were characteristic of the selected CoMFA, CoMSIA models. In progressive scrambling test, all the models had $dq^{2\prime}/dr^2_{yy\prime}$ values lower than 1.0 (not shown for shorting the paper), notarizing that the QSAR models obtained with the current data did not arose by haphazard.

3.2. Validation of QSAR models using external test set

The predictive power of the obtained models was further evaluated using the external test set of 28 molecules. The predicted versus measured pK_i values for the training and test sets were listed in Table 1 and depicted graphically in Fig. 3 for the CoMFA, CoMSIA models, respectively. As it was shown, most of the molecules were drawn on or near the diagonal line, which indicated good predictive abilities of both models. For the prediction of the external test set, CoMFA and CoMSIA model both showed a high degree of predictive power with pretty good r^2_{pre} values of 0.723 and 0.685, respectively. CoMFA model seemed better than the CoMSIA model in the prediction of the external test set in terms of the predictive r^2_{pre} value. Two molecules (114, 141) out of 28 test set molecules were badly predicted with residues more than 1.5 using the CoMFA model. The bad prediction of compound 114 might ascribe to its unique alkene double bond on the azabicycle [2,2,0] ring in the whole database. The bad prediction of compound 141 by CoMFA model was confusing because another similar compound 142 (different from compound 141 only in the 6-substitute) could be predicted well by CoMFA model. The 6-substitute effect probably was not well described in this CoMFA model. For the CoMSIA model, one training set molecule (3) and one test set molecule (156) were badly predicted with residues more than 1.5. The inferior predictive power of the CoMSIA model for compounds 3, 156 might ascribe to its less consideration of steric effect in the CoMSIA model.

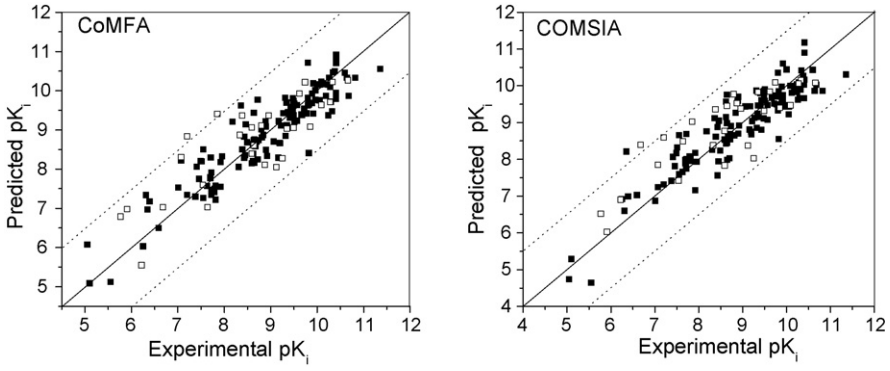

Fig. 3. Predicted vs. experimental binding affinity (pK_i) for the 158-nAChR ligands. (■) Training set and (□) test set. The solid line represents the ideal regression fitted line of the database molecules whereas the dotted line shows the error limit of ±1.5 log unit about the corresponding ideal fitted curve.

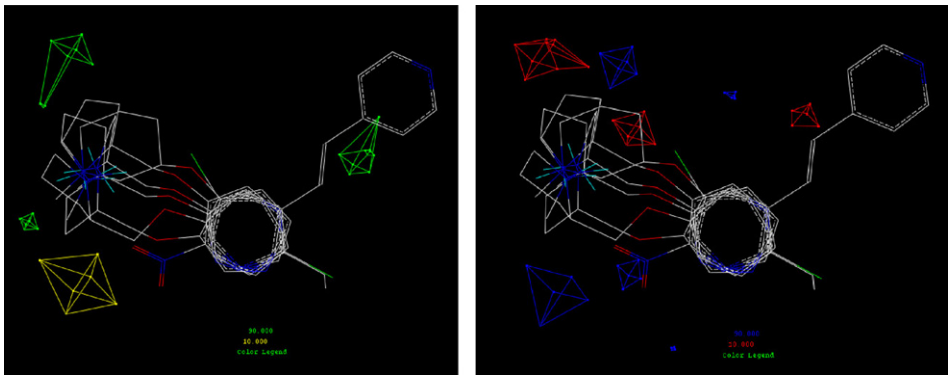

Fig. 4. Contour (“stdev × coeff”) plots of steric (left) and electrostatic (right) properties for the final CoMFA models in combination with exemplary compounds 5, 61, 73, 92, 117 and 132. Green contours indicate regions where an increase in steric bulk will enhance activity, and yellow contours indicate regions where an increase in steric bulk will reduce activity. Blue and red contours show regions of desirable positive and negative electrostatic interactions, respectively. The cutoff levels of contour are set at 90:10.

3.3. Graphics interpretation of QSAR models

In order to visualize the information of the derived 3D-QSAR model, the CoMFA and CoMSIA contour maps of the field contributions (“stdev × coeff”) of different properties were illustrated in the form of mesh using some exemplary compounds as reference structures in Figs. 4–6. The CoMFA contours highlight those areas where the ligands would interact with a possible environment, while CoMSIA isopleths lie within regions occupied by the ligands and denote those areas that favor or dislike the presence of a group with a particular physicochemical property [37]. The combined application of different methods enables one to verify the coincidence of the results or to complement either conclusion. To obtained a clearly look of important structural modulators of binding affinity, the cutoff threshold in contour plots were set to a ratio of 90:10 as favorable effect versus unfavorable effect.

3.3.1. CoMFA model

CoMFA steric and electrostatic PLS coefficient contributions for the pyridyl ether set of compounds are shown in Fig. 4. Green contours correspond to regions where more bulky group is good for enhancing affinity, while yellow contours correspond to regions where less bulky group is good. Blue and red contours show regions of desirable positive and negative electrostatic interactions, respectively.

Yellow isopleths were shown in the area down below the positive nitrogen of the heterocycle. Blue contours were also presented in this area. Groups with bulky volume and negative charge in this area would decrease the binding affinities. In the area opposite to the yellow area and in the area above the heterocycle, green contours were pictured which indicated that larger volume would help to improve the binding affinity. Red and blue contours were also shown above the heterocycle and near the 4-position of the pyrrolidine ring of compound 61, which indicated that an increasing affinity could also be expected by introducing a moderate negative group in this area. When we took a general view of the contour distributions near the heterocycle, we inferred that the area down below the nitrogen was located close to the direction of the interactions between the positive nitrogen and the nAChR receptor. As it was well known, the positive nitrogen on the heterocycle was played as a potent cation-π interaction site and an H-bond donor site when binding to the nAChR receptor [18,21,25,26]. Large bulky steric group near the interaction direction would hinder the nitrogen to fully interact with the receptor. More negative charged group near the interaction direction would weaken the cation-π interaction and the H-bond interaction

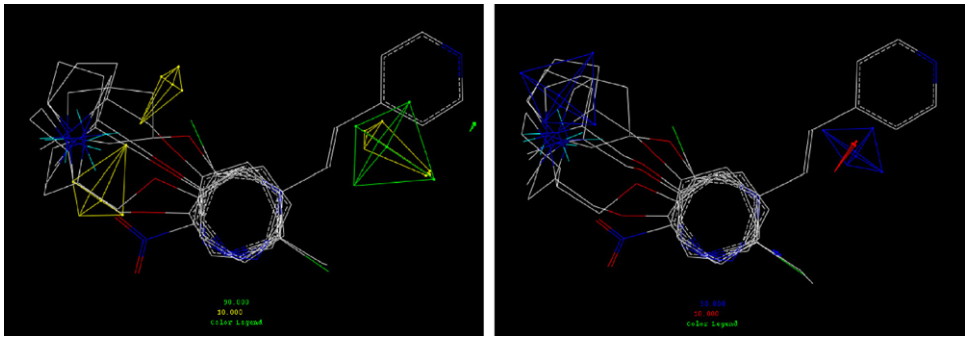

Fig. 5. Contour (“stdev × coeff”) plots of steric (left) and electrostatic (right) properties for the final CoMSIA models in combination with exemplary compounds 5, 61, 73, 92, 117 and 132. Green contours indicate regions where an increase in steric bulk will enhance activity, and yellow contours indicate regions where an increase in steric bulk will reduce activity. Blue and red contours show regions of desirable positive and negative electrostatic interactions, respectively. The cutoff levels of contour are set at 90:10.

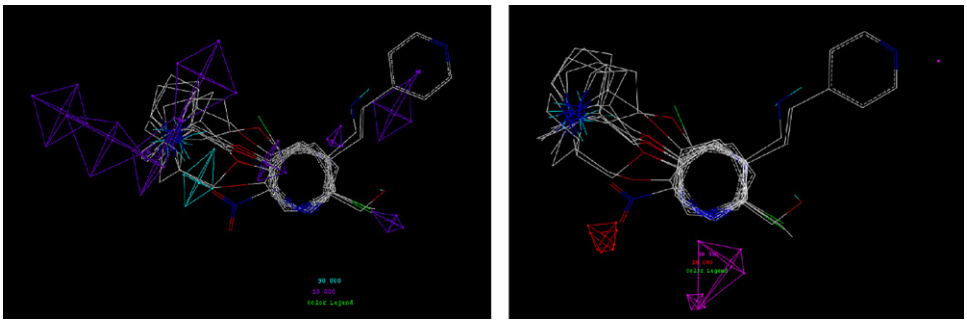

Fig. 6. Contour (''stdev × coeff'') plots of H-bond donor (left) and H-bond acceptor (right) fields for the final CoMSIA model in combination with exemplary compounds 5, 31, 61, 64, 73, 89, 92, 117 and 132. The presence of H-bond acceptor groups in the cyan areas increases binding affinity, whereas their presence in the purple area decreases binding affinity. The presence of H-bond donor groups in the magenta area increases binding affinity, whereas their presence in the red area decreases binding affinity. The cutoff levels of contour are set at 90:10.

thus resulted in lower affinity. For the other areas of the hererocyle apart from the interaction direction, their influence on the interaction was little. Larger volume would help to enhancing affinities by improving the van der Waals interaction between the hetercycle and the receptor. Moderate negative charged group could enhance the binding affinity by moderately increasing the positive charge on the positive nitrogen. Comparative or even higher affinities of the ligands with a pyrrolidine ring compared to the ligands with an azatidine ring might ascribe to this favorable steric effect. Similar conclusion was drawn in our previous study [23]. The red plot shown near the oxygen atom meant that introduction of more electronic density groups into these regions enhance the biological potency. This was coincident with the study of the Ferretti et al who suggested that the ether oxygen atom also contributed a lot to the affinity of pyridyl ethers [50].

The yellow area down below the nitrogen of the heterocyle was also extended to the area near the 2-substitute of the pyridine ring. Blue contours were also showed near the 2-substitute of the pyridine ring. Thus, the occupation of less bulky steric and more positive charged groups in this area would benefit improved affinity. The SAR analysis to the 2-substitute of pyridine ring also gave the same conclusion. The relative order of affinities was as following: $69 \approx 93 > 95 > 94$ ($H \approx F > CH_3 > Cl$), $113 > 112 > 111$ ($H > F > Cl$) and $1 > 2 > 3 > 4 \approx 6 > 5$ ($H > CH_3 > Br > SMe \approx I > NO_2$). As it can be seen, a reducing affinity was always observed for ligand whose 2-H was substituted with larger volume group. Steric effect seemed more influential than electronic effect on the affinities of the 2-substituted ligands. The study of Nicolotti et al. [21] also pointed out that there were a detrimental steric effects on the 2-position. Larger 2-substitute might hinder the nitrogen on the heterocycle ring to obtain the active conformer and result in dramatically reduced affinities. The best group on the 2-position should be the H atom.

A small blue area was shown in the upside of 4-substitute. Positive charged groups were suitable substitutes in this area. Thus, the very low affinity of compound 7 could be explained as the result of its rich electronic density group *N*,*N*-diethylamino carboxyl in this area. Same conclusion could be draw from the SAR analysis in this position, $8 > 9 > 7$ ($CH_3 > Br > CONEt_2$).

Green and red contours were shown near the double bond of 5-(pyrid-4-yl) vinyl substitute of compound 61. This indicated that a more bulky group or negative charged group there would increase biological activity. This explained the phenomenon that almost all ligands with a large aromatic group in this area processed a high affinity. When a general SAR analysis was performed on the 5-substitutes, it was found that 5-substitutes can tolerate a broad range of variation of steric and electrostatic properties. In addition, most of these analogues still possessed high affinities in the low nanomolar range. Consulting to the high affinities of the ligands with large or long chain aromatic 5-substitutes, we hypothesized that the 5-substitutes might direct to a relative roomy region in the ligand-binding domain of the receptor and little contact with the receptor, thus the immense changes of substitutes exerted minor influences on the ligand binding affinities.

3.3.2. CoMSIA model

The steric and electrostatic contour (''stdev × coeff'') plots of the final CoMSIA model are shown in Fig. 5. Yellow areas are shown between the nitric hetercycle and the pyridine ring. Any bulky occupation in these areas will harm the ligand affinity. Bulky steric group in this area may hinder this nitrogen from achieving active orientation, which will consequently lead to a reduced affinity of the ligand, such as compounds 131–153. These compounds tethered the methylene carbon into the ring, thus caused some degree of structural rigidity. A large blue area was lolled over the nitrogen of the pyrrolidine ring, which meant that more positive charge would enhance the binding affinity. This result was coincident with the localization of the heterocycle nitrogen in the crystallography structure [25,26]. In the crystal structure, the nitrogen was bury in an ''aromatic box'' consisted of six aromatic residues and interact with the residues through cation-π interaction. More positive heterocycle would help to increasing the binding affinity by enhancing the cation-π interaction.

To our surprise, confused steric and electronic contours were showed near the vinyl of 5-(pyrid-4-yl) vinyl substitute of compound 61. Green and yellow isopleths appeared almost at the same area. Blue and red isopleths were also shown in this area. It looked like it was a disputed region and the affinities of the compounds with the diverse structures indicated these variety. In

all positions of the pyridine ring of pyridyl ethers, the 5-position perhaps was investigated most thoroughly. However, the factors which modulate the affinity of the 5-substituted pyridyl ethers are still unclear. In former studies on pyridyl ethers [21,23], electronic effect [21] or steric effect [23] were showed to be close related with the binding affinity of 5-substituted ligands belonged to different classes, respectively. In another study [22], more 5-substituted ligands with diverse structures were correlated with their binding affinity. The best obtained model comprised of terms of hydrophobicity, molecular size and electronic density still could only explain 60% of the pK_i changes. Consulting to the above discussion of the CoMFA model, we could draw a conclusion that the 5-position should be orientated to a relative spacious region in the ligand binding domain of the nAChR receptor. In future's modification of 5-substitute, it should be pay attention not to introduce too large volume and too negative charged group, which would impair the complement between the 5-position and the ligand binding domain and resulted in lower affinity.

A small blue plot was show on the 6-substitute of pyridine ring, which indicated that positive group on the 6-postion would benefit to increase affinity. The SAR analysis of to the 6-substitute also gave the same conclusion. The relative order of affinities was as following: $27 < 30 < 28 < 29$ (F < Br < Me < Cl), **77** $< 73 = 74 < 75 \approx 76 < 72 = 70 \approx 69 < 68 < 71$ (Ph < Et = CN < OMe = vinyl < Me = F ≈ H < Cl < Br) and $106 < 104 < 102 < 103$ (OMe < Br < F < Me < Cl). As it can be seen, larger molecular size of the 6-substitute resulted in a lower binding affinity. The 6-substitute with rich density and large molecular size might interfere with the lone pair aromatic nitrogen in the formation of H-bond.

Fig. 6 shows the field contributions of the H-bond property of the final CoMSIA model. In principle, they should highlight areas beyond the ligands where putative hydrogen partners in the acceptor could form hydrogen bonds that influence binding affinity significantly. Favorable hydrogen bond donor and acceptor features on the ligand are colored in cyan and magenta, respectively, whereas the unfavorable regions are in purple and red, respectively.

The cyan area observed toward the added proton confirmed the importance of the H-bond donor property of the proton. Currently, there is still being debated about whether the protonated nitrogen should be defined as a hydrogen bond site in pharmacophoric elements of nAChR ligand. In the previous discussion, the H-bond property was also proved to be the most important modulator of the binding affinity. Thus, H-bond interaction should be regarded as one of the important interaction modes between the ligand and the receptor. Large purple areas were shown in the opposite area of the H-bond direction and upside the nitrogen of the heterocycle, which meant that any H-bond donor there would decrease the binding affinity. As to the pyridine ring, purple contours were shown in most of the position, such as the 3-position in the aromatic moiety, the adjacent area and the ulterior area of the 5-position, and the 6-substitute. In these areas, the introduction of group with H-bond donor property was bad to enhance the affinity. Examination of the SAR of the pyridine ring, the low affinities of compound 89 (5-CH_2NH_2) and 31 (6-CH_2OH) was resulted from the unfavorable H-bond donor property.

The H-bond acceptor contour plot clearly presented the H-bond acceptor site of ligand and H-bond donor site in receptor. The magenta contours near the nitrogen on pyridine ring showed that H-bond acceptor was favored at this position. This result was excellently in accordance with the currently pharmacophore model, in which the basic aromatic nitrogen was an important pharmacophoric element as H-bond acceptor. Furthermore, we could reasonably deduce that the situation of the aromatic nitrogen in the pyridine ring was very important for the binding of the nicotinic ligand. Only when the aromatic nitrogen was located on the meta-site of the group with a nitric heterocycle, can it be an effective H-bond donor. This conclusion has been observed in several studies [12,18,51,52]. Red plot were display in areas near 2-substitute of pyridine ring. Group with H-bond acceptor capability in the area would interfere the H-bond interaction between the positive nitrogen and the receptor, thus caused a reduced affinity. The low affinity of compound 5 (2-NO_2) might partially due to the unfavorable H-acceptor property of the NO_2.

4. Conclusion

CoMFA and CoMSIA techniques had been successfully applied to 158 nAChR ligands. Statistical significant models were obtained. The obtained models were satisfying based on both statistical significance and predictive ability, which suggested these models were robust enough for predicting novel ligands. However, the obtained CoMFA and CoMSIA differed from each other in terms of the contribution of physicochemical properties to the model. In the CoMFA model, steric effect was demonstrated to be the prevalent factor modulating the binding affinity of pyridyl ethers. Whereas, the CoMSIA model suggested that the determinant factor of the affinity was the H-bond interaction. This difference might arise from the principle applied in the CoMFA and CoMSIA techniques. We hypothesized that the CoMFA or CoMSIA model only explains part of the reasons of the total affinity variance in the whole database. Maybe, their combined application would practice more efficiently in guiding future synthesis.

Detailed information about structural modification was presented through different property contour plots from the final CoMFA and CoMSIA models. Some critical regions that regulated the binding strength of the pyridyl ether analogues have been pictured. Combined the crystal structures of the LBD of AChBP [25,26] and the obtained QSAR contours, a crude vision of the ligand localization in the binding pocket of receptor was obtained.

For the heterocycle moiety, the important substructure modulated the ligand binding was the protonated nitrogen. As is discussed above, the nitrogen of heterocycle was intimately interrelated with the ligands binding on the receptors. This result was agreement with the currently accepted localization of the protonated nitrogen of heterocycle in ligand binding domain of $\alpha4\beta2$ receptor, where the nitrogen buried in a pocket consisted of six aromatic residues and possibly interacted with

aromatic residues through cation-π interaction [25–35]. The protonated nitrogen was also acted as H-bond donor site in the ligand–receptor complex. In the area near the interaction direction, any bulky steric effect would impair the potential cation-π interaction and H-bond interaction. In other areas of the heterocycle apart from the interaction direction, large volume group would benefit to enhancing the ligand affinity because of the accretion of the van der Waals interaction between the ligand and the receptor. In addition, moderate negative charged group without H-bond donor properties in these areas would benefit to enhancing the cation-π interaction and H-bond interaction of the heterocycle nitrogen by improving the positive charge on the heterocycle.

For the pyridine ring moiety, the basic aromatic nitrogen served as H-bond acceptor, which was coincident with the pharmacophoric element of nAChR ligand. The relative localization of the aromatic nitrogen and the group with heterocycle was important to binding affinity of the pyridyl ethers. The aromatic nitrogen must be located on the meta-site of the group with heterocycle so that it can be act as an effective H-bond donor. Besides this, the 2-, 4-, 5- and 6-substitute of the pyridine ring all had strong impact on the ligand affinity. The 2-position of the pyridine ring was likely situated near the positive nitrogen of the heterocycle. Thus, the physicochemical property of the 2-substitute had strong influence on the binding affinity. The best suitable 2-substitutes should be less bulky steric and/or less negative charged group without H-bond acceptor property. The 4-postion of pyridine might be localized near the negative residues of the receptor, which demanded 4-substitute should be less negative charged. The 5-position seemed oriented toward such a spacious area that a suitable steric bulky group would favor to the increment of the affinity. Consulting to the docking structure of the A-85380 [29] and the crystal structure of nicotine-AChBP complex (pdb code: 1uw6) [26], we suggested that the 5-position was directed to the area surrounded by Thr144, His145, His146, Arg148, Glu149, Pro189 and Tyr192 of chain A (code in 1uw6) and Ser75, Leu102 and Arg104 of Chain B (code in 1uw6). This area was relative large and was lined with different physicochemical residues in the skirt. Therefore, the structure of 5-substitute could be changed in a broad range, while the resulted changes of their pK_i were in a small scope. Only when 5-substitute is large enough could it generate some specific interactions with complementary residues. For example, the high affinity of compound 61 was due to the specific interaction between its *para*-nitrogen on pyridine ring of the 5-(pyrid-4-yl) vinyl and Arg148 (code in 1uw6) on the receptor. In addition, it should also pay attention not to introduce group with H-bond donor properties to 5-substitute. The 6-position seemed be situated near the wall of the ligand binding domain. Limited space asked for the 6-substitute to be less bulky steric. In addition, the situation of the 6-substitute near the aromatic nitrogen also demanded a less negative charge group without H-bond acceptor capability.

In general, the combined application of CoMFA and CoMSIA techniques provide an efficient way to understand the possible interaction between the ligands and the receptors. Thus, more reasonable and meaningful information about structural modification were derived for design of novel, potent ligands. Further more, a crude vision of the ligand localization in the binding pocket of receptor was obtained. The result could be helpful to the docking study of ligands of 3-pyridyl ether analogues.

Acknowledgements

We are grateful to the Research Fund of the Ministry of Education of China for Homecoming Scholars and National Natural Science Foundation of China (No. 20671013). Furthermore, we would like to thank Mr. Hao He and ChemBay Technology Limited Company providing SGI workstation and related software for support.

Appendix A. Supplementary data

Supplementary data associated with this article can be found, in the online version, at doi:10.1016/j.jmgm.2006.11.005.

References

[1] M.W. Holladay, M.J. Dart, J.K. Lynch, Neuronal nicotinic acetylcholine receptors as targets for drug discovery, J. Med. Chem. 40 (1997) 4169–4194.
[2] M.W. Decker, J.D. Brioni, A.W. Bannon, et al., Diversity of neuronal nicotinic acetylcholine receptors: lessons from behavior and implications for CNS therapeutics, Life Sci. 56 (1995) 545–570.
[3] P.A. Newhouse, A. Potter, E.D. Levin, Nicotinic systems involvement in Alzheimer's and Parkinson's diseases: Implication for therapeutics, Drugs Aging 11 (1997) 206–228.
[4] G.K. Lloyd, M. Williams, Neuronal nicotinic acetylcholine receptors as novel drug targets, J. Pharmacol. Exp. Ther. 292 (2000) 461–467.
[5] S. Mihailescu, R. Drucker-Colýn, Nicotine, brain nicotinic receptors, and neuropsychiatric disorders, Arch. Med. Res. 31 (2000) 131–144.
[6] J.A. Dani, Overview of nicotinic receptors and their roles in the central nervous system, Biol. Psychiatry 49 (2001) 166–174.
[7] M.W. Decker, M.D. Meyer, J.P. Sullivan, The therapeutic potential of nicotinic acetylcholine receptor agonists for pain control, Expert. Opin. Investig. Drugs 10 (2001) 1819–1830.
[8] R.M. Novelloa, F. Gualtieri, Cholinergic nicotinic receptors: competitive ligands, allosteric modulatos, and their potential applications, Med. Res. Rev. 23 (2003) 393–426.
[9] R.A. Glennon, M. Dukat, Nicotine receptor ligands, Med. Chem. Res. 4 (1994) 461–473.
[10] M. Abreo, N.H. Lin, D. Garvey, et al., Novel 3-pyridyl ethers with subnanomolar affinity for central neuronal nicotinic acetylcholine receptors, J. Med. Chem. 39 (1996) 817–825.
[11] N.H. Lin, D.E. Gunn, Y. Li, Y. He, et al., Synthesis and structure–activity relationships of pyridine-modified analogs of 3-[2-((*S*)-pyrrolidinyl)-methoxy]pyridine, A-84543, a potent nicotinic acetylcholine receptor agonist, Bioorg. Med. Chem. Lett. 8 (1998) 248–254.
[12] N.H. Lin, M.A. Abreo, D.E. Gunn, S.A. Lebold, et al., Structure–activity studied on a novel series of cholinergic channel activators based on a heteroaryl ether framework, Bioorg. Med. Chem. Lett. 9 (1999) 2747–2752.
[13] N.H. Lin, Y. Li, Y. He, M.W. Holladay, T. Kuntzweiler, D.J. Anderson, et al., Synthesis and structure–activity relationships of 5-substituted pyridine analogues of 3-[2-((*S*)-pyrrolidinyl)methoxy]pyridine A-84543: a potent nicotinic receptor ligand, Bioorg. Med. Chem. Lett. 11 (2001) 631–633.
[14] N.H. Lin, L. Dong, W.H. Bunnelle, D.J. Anderson, M.D. Meyer, Synthesis and biological evaluation of pyridine-modified analogues of 3-(2-Aminoethoxy)pyridine as novel nicotinic receptor ligands, Bioorg. Med. Chem. Lett. 12 (2002) 3321–3324.

[15] G. Karig, J.M. Large, C.G.V. Sharples, A. Sutherland, T. Gallagher, et al., Synthesis and nicotinic binding of novel phenyl derivatives of UB-165. Identifying factors associated with α7 selectivity, Bioorg. Med. Chem. Lett. 13 (2003) 2825–2828.
[16] L.L. Brown, S. Kulkarni, O.A. Pavlova, A.O. Koren, et al., Synthesis and evaluation of a novel series of 2-chloro-5-((1-methyl-2-(*S*)-pyrrolidinyl)-methoxy)-3-(2-(4-pyridinyl)vinyl)pyridine analogues as potential positron emission tomography imaging agents for nicotinic acetylcholine receptors, J. Med. Chem. 45 (2002) 2841–2849.
[17] Y. Zhang, O.A. Pavlova, S.I. Chefer, A.W. Hall, V. Kurian, et al., 5-substituted drivatives of 6-hologeno-3-((2-(*S*)-azetidinyl)methoxyl)pyridine and 6-hologeno-hologeno-3-((2-(*S*)-pyrrolidinyl)methoxyl)pyridine with low picomolar affinity for α4β2 nicotinic acetylcholine receptor and wide range of lipophilicity: potential probes for imaging with positron emission tomography, J. Med. Chem. 47 (2004) 2453–2456.
[18] J.E. Tønder, P. Olesen, Agonists at the α4β2 nicotinic acetylcholine receptors: structure–activity relationships and molecular modeling, Curr. Med. Chem. 8 (2001) 651–674.
[19] J.E. Tønder, P. Olesen, J.B. Hansen, M. Begtrup, I.J. Petterson, An improved nicotinic pharmacophore and a stereoselective CoMFA-model for nicotinic agonists acting at the central nicotinic acetylcholine receptors labeled by [^{3}H]-*N*-methylcarbamylcholine, J. Comput. Aid. Mol. Des. 15 (2001) 247–258.
[20] O. Nicolotti, M. Pellegrini-calace, A. Carrieri, et al., Neuronal nicotinc receptor agonists: a multi-approach development of the pharmacophore, J. Comput. Aid. Mol. Des. 15 (2001) 859–872.
[21] O. Nicolotti, M. Pellegrini-Callace, C. Altomare, A. Cartotti, A. Carrieri, F. Sanz, Ligands of neuronal acetylcholine receptor (nAChR): inferences from the hansch and 3-D quantitative structure–activity relationship (QSAR) models, Curr. Med. Chem. 9 (2002) 1–29.
[22] O. Nicolotti, C. Altomare, Ma. Pellegrini-Calace, A. Carotti, Neuronal nicotinic acetylcholine receptor agonists: pharmacophores, evolutionary QSAR and 3D-QSAR models, Curr. Topics Med. Chem. 4 (2004) 335–360.
[23] H.B. Zhang, H. Li, C.P. Liu, CoMFA, CoMSIA, and molecular hologram QSAR studies of novel neuronal nAChRs ligands—open ring analogues of 3-pyridyl ether, J. Chem. Inf. Model. 45 (2005) 440–448.
[24] J.D. Schmitt, Exploring the nature of molecular recognition in nicotinic acetylcholine receptors, Curr. Med. Chem. 7 (2000) 749–800.
[25] K. Brejc, W.J. van Dijk, R.V. Klaassen, M. Schuurmans, J. van der Oost, A.B. Smit, T.K. Sixma, Crystal structure of an ACh-binding protein reveals the ligand-binding domain of nicotinic receptors, Nature 411 (2001) 269–276.
[26] P.H.N. Celie, S.E. Van Rossum-Fikkert, W.J. Van Dijk, K. Brejc, A.B. Smit, T.K. Sixma, Nicotine and carbamylcholine binding to nicotinic acetylcholine receptors as studied in AChBP crystal structure, Neuron 41 (2004) 907–914.
[27] A.L. Cashin, E.J. Petersson, H.A. Lester, D.A. Dougherty, Using physical chemistry to differentiate nicotinic from cholinergic agonists at the nicotinic acetylcholine receptor, J. Am. Chem. Soc. 127 (2005) 350–356.
[28] D.B. Tikhonov, L.R. Mellor, P.N.R. Usherwood, Modeling noncompetitive antagonism of a nicotinic acetylcholine receptor, Biophys. J. 87 (2004) 159–170.
[29] W.H. Bisson, L. Scapozza, G. Westera, L. Mu, P.A. Schubiger, Ligand selectivity for the acetylcholine binding site of the rat α4β2 and α3β4 nicotinic subtypes investigated by molecular docking, J. Med. Chem. 48 (2005) 5123–5130.
[30] R. Artali, G. Bombieri, F. Meneghetti, Docking of 6-chloropyridazin-3-yl derivatives active on nicotinic acetylcholine receptors into molluscan acetylcholine binding protein (AChBP), II Farmaco 60 (2005) 313–320.
[31] X.Q. Huang, F. Zheng, P.A. Crooks, L.P. Dwoskin, Ch.-G. Zhan, modeling multiple species of nicotine and deschloroepibatidine interacting with α4β2 nicotinic acetylcholine receptor: from microscopic binding to phenomenological binding affinity, J. Am. Chem. Soc. 127 (2005) 14401–14414.
[32] M. Schapira, R. Abagyan, M. Totrov, Structural model of nicotine acetylcholine receptor isotypes bound to acetylcholine and nicotine, BMC Struct. Biol. 2 (2002) 1–8.
[33] N. Le Novère, T. Grutter, J.P. Changeux, Models of the extracellular domain of the nicotinic receptors and of agonist- and Ca^{2+}-binding sites, Proc. Natl. Acad. Sci. U.S.A. 99 (2002) 3210–3215.
[34] C. Fruchart-Gaillard, B. Gilquin, S. Antil-Delbeke, et al., Experimentally based model of a complex between a snake toxin and the a7 nicotinic receptor, Proc. Natl. Acad. Sci. U.S.A. 99 (2002) 3216–3221.
[35] V. Costa, A. Nistri, A. Cavalli, P. Carloni, A structural model of agonist binding to the alpha3beta4 neuronal nicotinic receptor, Br. J. Pharmacol. 140 (2003) 921–931.
[36] M. Clark, R.D. Cramer, D.M. Jones, D.E. Patterson, P.E. Simeroth, Comparative molecular field analysis (CoMFA). 2. Toward its use with 3D-structural databases, Tetrahedron Comput. Methodol. 3 (1990) 47–59.
[37] G. Klebe, U. Abraham, T. Mietzner, Molecular similarity indices in a comparative analysis (CoMSIA) of drug molecules to correlate and predict their biological activity, J. Med. Chem. 37 (1994) 4130–4136.
[38] L.L. Brown, O. Pavlova, A. Mukhin, A.S. Kimes, A.G. Horti, Radiosynthesis of 5-(2-(4-pyridinyl)vinyl)-6-chloro-3-(1-[(11)C]methyl-2-(*S*)-pyrrolidinylmethoxy)pyridine, a high affinity ligand for studying nicotinic acetylcholine receptors by positron emission tomography, Bioorg. Med. Chem. 9 (2001) 3055–3058.
[39] M.W. Holladay, J.T. Wasicak, N.H. Lin, Y. He, et al., Identification and initial structure–activity relationships of (*R*)-5-(2-azetidinylmethoxy)-2-chloropyridine (ABT-594), a potent, orally active, non-opiate analgesic agent acting via neuronal nicotinic acetylcholine receptors, J. Med. Chem. 41 (1998) 407–412.
[40] M.W. Holladay, H. Bai, Y. Li, N.H. Lin, J.F. Daanen, K.B. Ryther, et al., Structure–activity studies related to ABT-594, a potent nonopioid analgesic agent: effect of pyridine and azetidine ring substitutions on nicotinic acetylcholine receptor binding affinity and analgesic activity in mice, Bioorg. Med. Chem. Lett. 8 (1998) 2797–2802.
[41] G.R. Krow, J. Yuan, Y. Fang, M.D. Meyer, D.J. Anderson, J.E. Campbell, P.J. Carroll, Synthesis of 3- and 5-endo-(6-chloro-3-pyridoxy)-methyl-2-azabicyclo[2.2.0]hexane and 3-endo-(6-chloro-3-pyridoxy)-methyl-2-azabicyclo[2.2.0]hex-5-ene. ABT 594 analogs, Tetrahedron 56 (2000) 9227–9232.
[42] J. Lee, C.B. Davis, R.A. Rivero, A.B. Reitz, R.P. Shank, Synthesis and structure–activity relationship of novel pyridyl ethers for the nicotinic acetylcholine receptor, Bioorg. Med. Chem. Lett. 10 (2000) 1063–1066.
[43] S.L. Jung, Pyridyl Ethers and Thioethers as Ligands for Nicotinic Acetylcholine Receptor and its Therapeutic Application, United States patent application publication. Patent No. US 2003/0207858 (2003).
[44] M.J. Dart, J.T. Wasicak, K.B. Ryther, M.R. Schrimpf, K.H. Kim, D.J. Anderson, J.P. Sullivan, M.D. Meyer, Structural aspects of high affinity ligands for the alpha 4 beta 2 neuronal nicotinic receptor, Pharm. Acta Helv. 74 (2000) 115–123.
[45] S.F. Nielsen, E.Ø. Nielsen, G.M. Olsen, T. Liljefors, D. Peters, Novel potent ligands for the central nicotinic acetylcholine receptor: synthesis, receptor binding, and 3D-QSAR analyses, J. Med. Chem. 43 (2000) 2217–2226.
[46] Sybyl Version 6.91, Tripos Inc., 1699 Hanley Road, St. Louis.
[47] G. Ferretti, M. Dukat, M. Giannella, A. Piergentili, et al., Homoazanicotine: a structure-affinity study for nicotinic acetylcholine (nACh) receptor binding, J. Med. Chem. 45 (2002) 4724–4731.
[48] B.L. Bush, R.B. Nachbar, Sample-distance partial least squares: PLS optimized for many variables, with application to CoMFA, J. Comput. Aid. Mol. Des. 7 (1993) 587–619.
[49] R.D. Clark, D.G. Sprous, J.M. Leonard, Validating Models Based on Large Data Sets. Rational Approaches to Drug Design, Prous Science SA, Barcelona, 2001, pp. 475–485.
[50] G. Ferretti, M. Dukat, M. Giannella, A. Piergentili, et al., Homoazanicotine: a structure-affinity study for nicotinic acetylcholine (nACh) receptor binding, J. Med. Chem. 45 (2002) 4724–4731.
[51] R.A. Glennon, M. Dukat, L. Liao, Musings on α4β2 nicotinic acetylcholine (nACh) receptor pharmacophore models, Curr. Topics Med. Chem. 4 (2004) 631–644.
[52] H.B. Zhang, C.P. Liu, H. Li, CoMFA and CoMSIA studies of nAChRs ligands: epibatidine analogues, QSAR Comb. Sci. 23 (2004) 80–88.